The Astrophysical Journal, 591:L95–L98, 2003 July 10

LARGE DISKLIKE GALAXIES AT HIGH REDSHIFT[1]

Ivo Labbé,[2] Gregory Rudnick,[3] Marijn Franx,[2] Emanuele Daddi,[4] Pieter G. van Dokkum,[5] Natascha M. Förster Schreiber,[2] Konrad Kuijken,[2] Alan Moorwood,[5] Hans-Walter Rix,[6] Huub Röttgering,[2] Ignacio Trujillo,[4] Arjen van der Wel,[2] Paul van der Werf,[2] and Lottie van Starkenburg[2]

Received 2003 April 28; accepted 2003 May 28; published 2003 June 13

ABSTRACT

Using deep near-infrared imaging of the Hubble Deep Field–South with the Infrared Spectrometer and Array Camera on the Very Large Telescope, we find six large disklike galaxies at redshifts $z = 1.4$–3.0. The galaxies, selected in K_s (2.2 μm), are regular and surprisingly large in the near-infrared (rest-frame optical), with face-on effective radii $r_e = 0\farcs65$–$0\farcs9$ or 5.0–7.5 h_{70}^{-1} kpc in a Λ cold dark matter cosmology, comparable to the Milky Way. The surface brightness profiles are consistent with an exponential law over 2–3 effective radii. The Wide Field Planetary Camera 2 morphologies in *Hubble Space Telescope* imaging (rest-frame UV) are irregular and show complex aggregates of star-forming regions $\sim 2''$ ($\sim 15\ h_{70}^{-1}$ kpc) across, symmetrically distributed around the K_s-band centers. The spectral energy distributions show clear breaks in the rest-frame optical. The breaks are strongest in the central regions of the galaxies and can be identified as the age-sensitive Balmer/4000 Å break. The most straightforward interpretation is that these galaxies are large disk galaxies; deep near-infrared data are indispensable for this classification. The candidate disks constitute 50% of galaxies with $L_V \gtrsim 6 \times 10^{10}\ h_{70}^{-2}\ L_\odot$ at $z = 1.4$–3.0. This discovery was not expected on the basis of previously studied samples. In particular, the Hubble Deep Field–North is deficient in large galaxies with the morphologies and profiles we report here.

Subject headings: galaxies: evolution — galaxies: high-redshift — infrared: galaxies

1. INTRODUCTION

Disk galaxies are believed to undergo a relatively simple formation process in which gas cools and contracts in dark matter halos to form rotationally supported disks with exponential light profiles (Fall & Efstathiou 1980; Mo, Mao, & White 1998). A critical test of any theory of galaxy formation is to reproduce the observed properties and evolution of galaxy disks.

Previous optical spectroscopy and *Hubble Space Telescope* (*HST*) imaging have yielded a wealth of data on disk galaxies at $z \lesssim 1$ (e.g., Vogt et al. 1996, 1997; Lilly et al. 1998; Barden et al. 2003), although contradictory claims have been made regarding the implications for the size and luminosity evolution with redshift (see Lilly et al. 1998; Mao, Mo, & White 1998; Barden et al. 2003) and the importance of surface brightness selection effects (see Simard et al. 1999 and Bouwens & Silk 2002).

It is still unknown what the space density and properties are of disk galaxies at substantially higher redshift. Many galaxies at $z \sim 3$ have been identified using the efficient *U*-dropout technique (Steidel et al. 1996a, 1996b). Most of these objects are compact with radii $\sim$1–2 h_{70}^{-1} kpc, but some are large and irregular (Giavalisco, Steidel, & Macchetto 1996; Lowenthal et al. 1997). However, the *U*-drop selection requires high far-UV surface brightness because of active, spatially compact, and unobscured star formation. As a result, large and UV-faint disk galaxies may have been overlooked, and, additionally, the morphologies of Lyman break galaxies (LBGs) could just reveal the unobscured star-forming regions rather than the more evolved underlying population that forms the disk.

The most direct evidence for the existence of large disks at high redshift has come from observations in the near-infrared (NIR), which provide access to the rest-frame optical. Here the continuum light is more indicative of the distribution of stellar mass than in the UV, and nebular lines are accessible for kinematic measurements. Van Dokkum & Stanford (2001) discuss a *K*-selected galaxy at $z = 1.34$ with a rotation velocity of $\sim$290 km s^{-1}. Erb et al. (2003) detect an $\sim$150 km s^{-1} rotation at $\sim 6\ h_{70}^{-1}$ kpc radii in the Hα emission line of galaxies at $z \sim 2.3$, and Moorwood et al. (2003) find $\gtrsim$100 km s^{-1} rotation at $\sim 6\ h_{70}^{-1}$ kpc from the center of a galaxy at $z = 3.2$, seen in the NIR spectrum of the [O III] λ5007 emission line.

The imaging data in these studies, however, are of limited depth and resolution, making it difficult to determine morphological properties. In this Letter, we present an analysis of the rest-frame ultraviolet-to-optical morphologies and spectral energy distributions (SEDs) of six large candidate disk galaxies at $z \sim 1.4$–3 using the deepest ground-based NIR data set currently available (Labbé et al. 2003). Throughout, we adopt a flat Λ-dominated cosmology ($\Omega_M = 0.3$, $\Lambda = 0.7$, and $H_0 = 70\ h_{70}$ km s^{-1} Mpc^{-1}). All magnitudes are expressed in the Johnson photometric system.

2. OBSERVATIONS

We obtained 102 hr of NIR J_s, H, and K_s imaging in the Hubble Deep Field–South (HDF-S; $2\farcm5 \times 2\farcm5$) under excellent seeing (FWHM $\approx 0\farcs46$), using the Infrared Spectrometer and Array Camera (ISAAC; Moorwood 1997) on the Very Large Telescope (VLT). The observations were taken as part of the

[1] Based on service mode observations collected at the European Southern Observatory, Paranal, Chile (ESO programme 164.O-0612) and also based on observations with the NASA/ESA *Hubble Space Telescope*, obtained at the Space Telescope Science Institute, which is operated by AURA, Inc., under NASA contract NAS5-26555.

[2] Leiden Observatory, P.O. Box 9513, NL-2300 RA Leiden, Netherlands.
[3] Max-Plank-Institut für Astrophysik, Karl-Schwarzschild-Strasse 1, Postfach 1317, D-85741 Garching, Germany.
[4] European Southern Observatory, Karl-Schwarzschild-Strasse 2, D-85748 Garching, Germany.
[5] Department of Astronomy, Yale University, P.O. Box 208101, New Haven, CT 06520-8101.
[6] Max-Plank-Institut für Astronomie, Koenigstuhl 17, D-69117 Heidelberg, Germany.

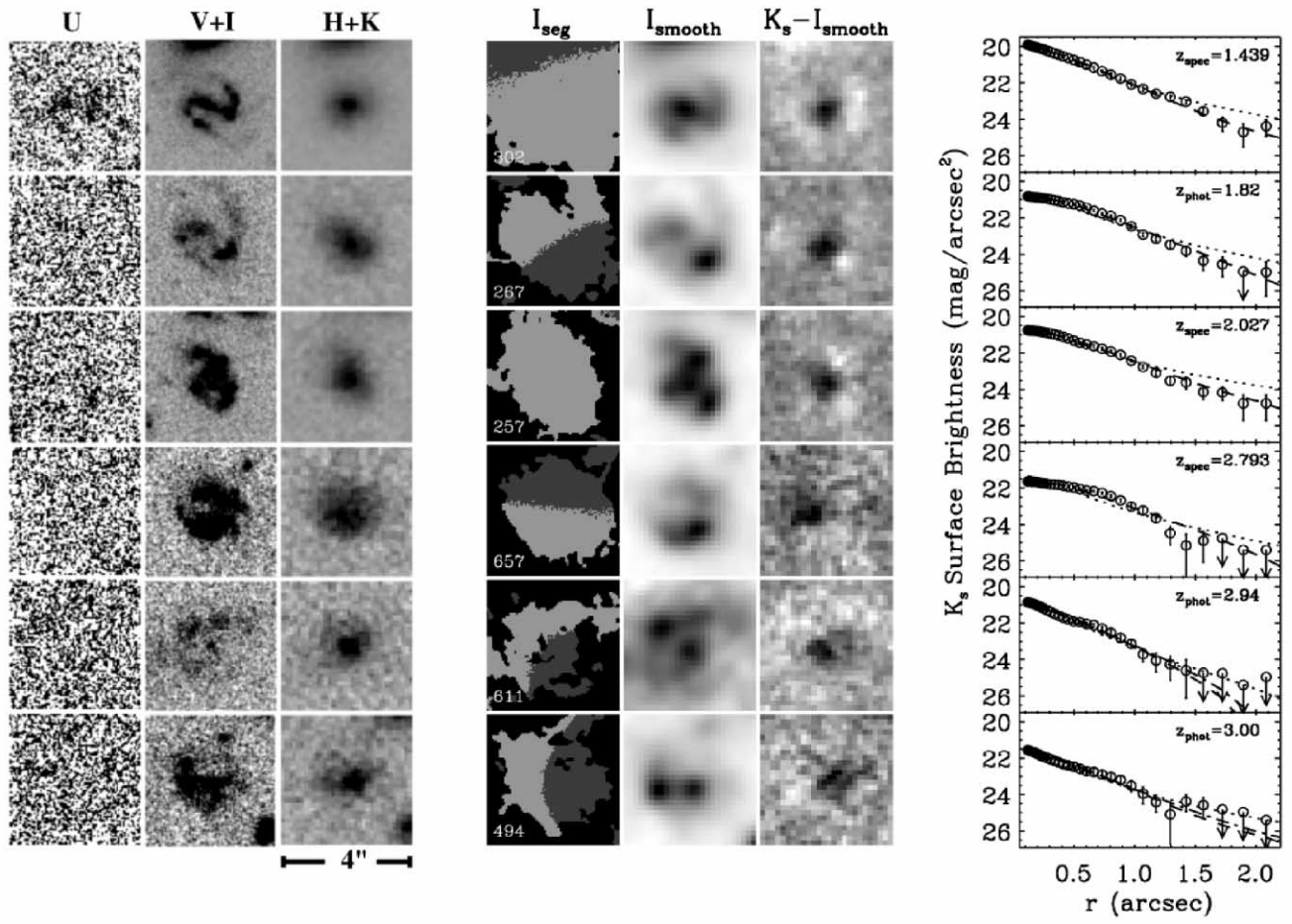

FIG. 1.—*Left panels:* WFPC2 U_{300}, averaged $V_{606} + I_{814}$ (rest-frame UV), and our averaged ISAAC $H + K_s$ images (rest-frame optical), scaled proportional to F_λ with arbitrary normalization per galaxy. The rest-frame UV morphologies are complex and symmetric with respect to the center of the smoother optical distribution. *Middle panels:* SExtractor's I_{814}-band segmentation map, the smoothed I_{814} images, and the K_s-band images after subtracting the scaled, smoothed I_{814} band. From the segmentation map, it follows that detection in I_{814} would likely split up most of the sources. The central residuals in $K_s - I_{smooth}$ demonstrate that optical and NIR light are distributed differently and that all galaxies have a "red" nucleus. *Right panels:* Radial profiles in the K_s band. The abscissa and the ordinate are, respectively, the mean geometric radial distance and the surface brightness along elliptical isophotes. The arrows mark 1 σ confidence intervals for measurements with a signal-to-noise ratio of less than 1. Overplotted are the best-fit exponential law (*dashed line*), $r^{1/4}$ law (*dotted line*), and point+exponential (*dash-dotted line*) for galaxies 494 and 611.

Faint InfraRed Extragalactic Survey (FIRES; Franx et al. 2000). We combined our data with existing deep optical *HST*/Wide Field Planetary Camera 2 (WFPC2) imaging (ver. 2; Casertano et al. 2000), in the U_{300}, B_{450}, V_{606}, and I_{814} bands, and we assembled a K_s-selected catalog of sources with SExtractor (Bertin & Arnouts 1996). Photometric redshifts and rest-frame luminosities were derived by fitting a linear combination of empirical galaxy spectra and stellar population models to the observed flux points (Rudnick et al. 2001; G. Rudnick et al. 2003a, in preparation). The reduced images, photometric catalog, and redshifts are presented in Labbé et al. (2003) and are all available on-line at the FIRES home page.[7] Furthermore, we obtained optical spectroscopy with FORS1 on the VLT for some of the sources (G. Rudnick et al. 2003b, in preparation). Additional redshifts were obtained from Vanzella et al. (2002). As discussed in Rudnick et al. (2001; G. Rudnick et al. 2003a, in preparation), our photometric redshifts yield good agreement with the spectroscopic redshifts, with an rms of $|z_{spec} - z_{phot}|/(1 + z_{spec}) \approx 0.05$ for $z_{spec} > 1.4$.

Large disk galaxies in the HDF-S were identified by fitting exponential profiles convolved with the point-spread function (PSF) to the K_s-band images. Six objects at $z > 1.4$ have effective radii $r_e > 3.6\ h_{70}^{-1}$ kpc, three of which have spectroscopic redshifts. The mean redshift of the sample is 2.4. We will focus on these large galaxies in the remainder of the Letter. The structural properties of the full K_s-selected sample will be discussed in I. Trujillo et al. (2003, in preparation).

3. REST-FRAME OPTICAL VERSUS UV MORPHOLOGY

The large galaxies are shown in Figure 1. They have a regular morphology in the ISAAC K_s band (2.2 μm), which probes rest-frame optical wavelengths between 5400 and 9000 Å. In contrast, the WFPC2 V_{606}- and I_{814}-band morphologies, which map the unobscured star-forming regions at rest-frame UV wavelengths between 1500 and 3300 Å, are irregular with several knots up to ~2″ (~15 h_{70}^{-1} kpc) apart, symmetrically distributed around the K_s-band centers. In a few cases, the observed optical light is spatially almost distinct from the NIR.

As a result of the structure in the WFPC2 imaging, four of the large objects have been split up into two sources by Casertano et al. (2000). Figure 1 shows the corresponding "segmentation" map by "SExtractor" that illustrates how the pixels in each image are allocated to different sources. The galaxies

[7] See http://www.strw.leidenuniv.nl/~fires.

TABLE 1
PROPERTIES OF HIGH-REDSHIFT DISK GALAXIES IN THE HDF-S

Galaxy (1)	$K_{s,\,tot}$ (2)	z (3)	$M_{B,\,rest}$ (4)	$\mu_{0,\,B,\,rest}$ (5)	$r_{e,\,K}$ (arcsec) (6)	$r_{1/2,\,K}$ (arcsec) (7)	$r_{1/2,\,I}$ (arcsec) (8)	ϵ (9)
302	19.70	1.439[a]	−22.70	19.70	0.89	0.70	0.86	0.46
267	19.98	1.82	−22.88	19.92	0.75	0.74	0.88	0.37
257	20.25	2.027[a]	−23.08	19.53	0.74	0.74	0.84	0.36
657	20.68	2.793[a]	−23.56	19.33	0.76	0.70	0.74	0.18
611	20.53	2.94	−23.59	18.51	0.65[b]	0.52	0.97	0.27
494	21.14	3.00	−23.31	18.84	0.75[b]	0.56	0.86	0.47

NOTE.—Col. (1): Catalog identification numbers (see Labbé et al. 2003). Col. (2): K_s-band total magnitudes. Col. (3): Redshift. Col. (4): Rest-frame absolute B-band magnitudes. Col. (5): Face-on rest-frame B-band central surface brightnesses. Col. (6): Face-on best-fit effective radii. Col. (7): K_s half-light radii. Col. (8): I_{814} half-light radii, PSF-matched to K_s. Col. (9): Ellipticity.
[a] Spectroscopic redshifts.
[b] Two-component models (point+exponential).

were not split up when the K_s-band image was used to detect objects. However, the broader PSF in the K_s-band image can play a role: if we smooth the I_{814}-band data to the same resolution, we find that SExtractor only splits up one galaxy.

Hence, the question remains whether these four objects split up in I_{814} are superpositions or whether they are part of larger systems. We tested this by subtracting the PSF-matched I_{814}-band images from the K_s-band images. The I_{814}-band images were scaled to the K_s-band images to minimize the residuals. The residuals are shown in Figure 1. In all cases, we find strong positive residuals close to the centers of the objects as defined in the K_s-band, whereas residuals at any of the I_{814}-band peaks might be expected in case of a chance superposition. Furthermore, we performed photometric redshift analyses for subsections of the images and found no evidence of components at different redshifts.

4. PROFILE FITS AND SIZES

Next, we fitted simple models convolved with the PSF (FWHM ≈ 0.″46) to the two-dimensional surface brightness distributions in the K_s band. The images are well described by a simple exponential law over 2–3 effective radii (galaxies 302, 267, 257, and 657) or by a point source plus exponential (galaxies 611 and 494), where the point source presumably represents the light emitted by a compact bulge contributing about 40% of the light. We also derived intensity profiles by ellipse fitting. As can be seen in Figure 1, most galaxies are well described by an exponential. The central surface brightnesses and effective radii, enclosing half of the flux of the model profile, are corrected to face-on and are shown in Table 1. The central surface brightness is multiplied with $(1-\epsilon)^{1/2}$, as an intermediate case between optically thin and optically thick, and corrected for cosmological dimming.

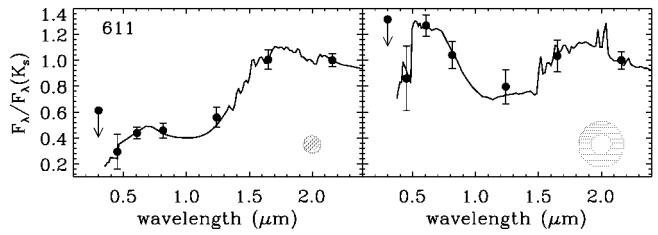

FIG. 2.—SED of source 611 in a 0.″7 circular diameter aperture (*left*) and in a concentric 1″–2″ diameter ring (*right*), normalized to the K_s-band flux. Overplotted are independent model fits from G. Rudnick et al. (2003a, in preparation).

The effective radii (semimajor axes) are surprisingly large, $r_e = 0.''65$–$0.''9$ (5.0–7.5 h_{70}^{-1} kpc in a Λ cold dark matter [ΛCDM] cosmology), comparable to the Milky Way and much larger than typical sizes of "normal" LBGs (Giavalisco et al. 1996; Lowenthal et al. 1997). As might be expected from the previous section, the I-band images have even larger effective radii. All galaxies have a "red" nucleus, and the colors become bluer in the outer parts.

Overall, the optical-to-infrared morphologies and sizes are strikingly similar to L^* disk galaxies in the local universe, with red bulges, more diffuse bluer exponential disks, and scattered UV-bright star-forming regions. Some even show evidence of well-developed grand-design spiral structure. However, the mean central surface brightness of the disks is 1–2 mag higher than that of nearby disk galaxies, and the mean rest-frame color $(U-V) \approx 0$ is ∼1 mag bluer (see Lilly et al. 1998). Passive evolution can lead to disks with normal surface brightnesses at low redshift. Alternatively, the disks are disrupted later by interactions or evolve into S0 galaxies, which have higher surface brightnesses (e.g., Burstein 1979).

5. SPECTRAL ENERGY DISTRIBUTION

The overall SEDs of the galaxies show a large variety. Four of the galaxies (257, 267, 494, and 657) satisfy conventional U-dropout criteria (Madau et al. 1996; Giavalisco & Dickinson 2001). One galaxy is at too low redshift (302) to be classified as a U-dropout, and one other galaxy is too faint in the rest-frame UV (611). It has $J_s-K_s > 2.3$ and is part of the population of evolved galaxies identified by Franx et al. (2003) and van Dokkum et al. (2003).

The red colors of the central components can be due to either dust, higher age, emission-line contamination, or a combination of effects. The SEDs show stronger Balmer/4000 Å breaks in the inner parts than in the outer parts (see Fig. 2 for an example). We derived colors inside and outside of a 0.″7 radius centered on the K_s-band center. The mean differences are ∼0.5 mag in observed $I_{814}-K_s$ and ∼0.2 mag in rest-frame $U-V$. Higher resolution Near-Infrared Camera and Multi-Object Spectrometer data are required to address the population differences in more detail.

6. DISCUSSION

We have found six large galaxies with characteristics similar to those of nearby disk galaxies: exponential profiles with large-scale lengths, more regular and centrally concentrated morphologies in the rest-frame optical than in the rest-frame UV,

and, as a result, red nuclei. It is very tempting to classify these galaxies as disk galaxies, given the similarities with low-redshift disk galaxies. However, kinematic studies are necessary to confirm that the material is in a rotating disk. Photometric studies of larger samples are needed to constrain the thickness of the disks. We note that the simulations of Steinmetz & Navarro (2002) can show extended structures during a merging or accretion event. However, the expected duration of this phase is short, and the disk galaxies comprise a high fraction of the bright objects. It is therefore unlikely that a significant fraction of the galaxies presented here are undergoing such an event.

The density of these large disk galaxies is fairly low: over a survey area of 4.7 arcmin^2 and to a magnitude limit of $K_{s,\,\mathrm{tot}} = 22$, they make up six out of 52 galaxies at $1.4 \leqslant z \leqslant 3.0$. However, they do constitute six out of the 12 most rest-frame–luminous galaxies $L_V \gtrsim 6 \times 10^{10}\ h_{70}^{-2}\ L_\odot$ in the same redshift range. The comoving volume density is $\sim 3 \times 10^{-4}\ h_{70}^{3}$ Mpc^{-3} at a mean redshift $z \approx 2.3$. Obviously, larger area surveys are needed to establish the true density. We note that three of the galaxies have only photometric redshifts, one of which (a *U*-drop galaxy at $z_{\mathrm{phot}} = 1.82$) is in the poorly tested range $1.4 < z < 2.0$. The volume density of disk galaxies with $r_e > 3.6\ h_{70}^{-1}$ kpc in the local universe is much higher at $\sim 3 \times 10^{-3}\ h_{70}^{3}$ Mpc^{-3} (de Jong 1996), although many nearby disks would not be present in our high-redshift sample because their surface brightness would be too low.

We note that similar galaxies are absent in the very deep NIR imaging data on the Hubble Deep Field–North (HDF-N; Williams et al. 1996; Dickinson 2000). Although notable differences between optical and NIR morphologies were reported for two of the largest LBGs in the HDF-N, no large galaxies were reported to have red nuclei or exponential profiles as in the HDF-S. The two fields are different in other aspects as well. We found earlier that the HDF-N is deficient in red sources (e.g., Labbé et al. 2003 vs. Papovich, Dickinson, & Ferguson 2001) and that the disk galaxies are more luminous in the *H* band than most of the high-redshift galaxies found in the HDF-N (Papovich et al. 2001). The larger number of red galaxies in the HDF-S (e.g., Labbé et al. 2003; Franx et al. 2003) and their strong clustering (Daddi et al. 2003) may indicate that the red galaxies and large disks are both part of the same structures with high overdensities and evolve into the highest overdensities at low redshift, i.e., clusters. If this is the case, the large disk galaxies may be the progenitors of large S0 galaxies in the nearby clusters, which have colors very similar to elliptical galaxies (e.g., Bower, Lucey, & Ellis 1992).

Finally, we can compare the observed disk sizes with theoretical predictions. It is often assumed (Fall & Efstathiou 1980; Mo et al. 1998) that the disk scale length is determined by the spin parameter λ and the circular velocity of the virialized dark matter halo (Fall & Efstathiou 1980; Mo et al. 1998). For a ΛCDM cosmology, Mo, Mao, & White (1999) predict that the $z \sim 3$ space density of large ($r_e \gtrsim 3.6\ h_{70}^{-1}$ kpc) bright *U*-dropouts is $1.1 \times 10^{-4}\ h_{70}^{3}$ Mpc^{-3}, whereas we find that it is $\sim 2 \times 10^{-4}\ h_{70}^{3}$ Mpc^{-3} for our four *U*-drops at a mean $\langle z \rangle \sim 2.4$. This difference of a factor of 2 is not very significant, given our low number statistics and small survey volume. The combination of sizes and rotation velocities will give much stronger constraints on these models; it may be possible to measure the kinematics of some of these large galaxies using NIR spectrographs on large telescopes.

We thank the staff at ESO for their hard work in taking these data and making them available. This research was supported by grants from the Netherlands Foundation for Research (NWO), the Leids Kerkhoven-Bosscha Fonds, and the Lorentz Center. G. R. thanks Frank van den Bosch and Jarle Brinchmann for their useful discussions.

REFERENCES

Barden, M., Lehnert, M. D., Tacconi, L., Genzel, R., White, S., & Franceschini, A. 2003, ApJ, submitted (astro-ph/0302392)
Bertin, E., & Arnouts, S. 1996, A&AS, 117, 393
Bouwens, R., & Silk, J. 2002, ApJ, 568, 522
Bower, R. G., Lucey, J. R., & Ellis, R. S. 1992, MNRAS, 254, 601
Burstein, D. 1979, ApJ, 234, 435
Casertano, S., et al. 2000, AJ, 120, 2747
Daddi, E., et al. 2003, ApJ, 588, 50
de Jong, R. S. 1996, A&A, 313, 45
Dickinson, M. 2000, Philos. Trans. R. Soc. London, A358, 2001
Erb, D. K., Shapley, A. E., Steidal, C. C., Pettini, M., Adelberger, K. L., Hunt, M. P., Moorwood, A. F. M., & Cuby, J.-G. 2003, ApJ, 591, 101
Fall, S. M., & Efstathiou, G. 1980, MNRAS, 193, 189
Franx, M., et al. 2003, ApJ, 587, L79
———. 2000, Messenger, 99, 20
Giavalisco, M., & Dickinson, M. 2001, ApJ, 550, 177
Giavalisco, M., Steidel, C. C., & Macchetto, F. D. 1996, ApJ, 470, 189
Labbé, I., et al. 2003, AJ, 125, 1107
Lilly, S., et al. 1998, ApJ, 500, 75
Lowenthal, J. D., et al. 1997, ApJ, 481, 673
Madau, P., Ferguson, H. C., Dickinson, M. E., Giavalisco, M., Steidel, C. C., & Fruchter, A. 1996, MNRAS, 283, 1388
Mao, S., Mo, H. J., & White, S. D. M. 1998, MNRAS, 297, L71
Mo, H. J., Mao, S., & White, S. D. M. 1998, MNRAS, 295, 319
———. 1999, MNRAS, 304, 175
Moorwood, A. F. 1997, Proc. SPIE, 2871, 1146
Moorwood, A., van der Werf, P., Cuby, J.-G., & Oliva, T. 2003, in Proc. Workshop on the Mass of Galaxies at Low and High Redshift, ed. R. Bender & A. Renzini (New York: Springer), 302
Papovich, C., Dickinson, M., & Ferguson, H. C. 2001, ApJ, 559, 620
Rudnick, G. et al. 2001, AJ, 122, 2205
Simard, L., et al. 1999, ApJ, 519, 563
Steidel, C. C., Giavalisco, M., Dickinson, M., & Adelberger, K. L. 1996a, AJ, 112, 352
Steidel, C. C., Giavalisco, M., Pettini, M., Dickinson, M., & Adelberger, K. L. 1996b, ApJ, 462, L17
Steinmetz, M., & Navarro, J. F. 2002, NewA, 7, 155
van Dokkum, P. G., et al. 2003, ApJ, 587, L83
van Dokkum, P. G., & Stanford, S. A. 2001, ApJ, 562, L35
Vanzella, E., et al. 2002, A&A, 396, 847
Vogt, N. P., Forbes, D. A., Phillips, A. C., Gronwall, C., Faber, S. M., Illingworth, G. D., & Koo, D. C. 1996, ApJ, 465, L15
Vogt, N. P., et al. 1997, ApJ, 479, L121
Williams, R. E., et al. 1996, AJ, 112, 1335